ISSN : 2355-9365 e-Proceeding of Engineering : Vol.13, No.3 Juni 2026 | Page 1342

Detection Of Surface Elevation And River Flow Velocity Using A Milimeter Wace Fmcw Radar System

Writer Lutvi Adam Harahap
Faculty of Electrical Engineering
Telkom University
Bandung, Indonesia
lutvihrp@telkomuniversity.ac.id

Husna Firyal Az-Zahra
Faculty of Electrical Engineering
Telkom University
Bandung, Indonesia
husnafrylazz@telkomuniversity.ac.id

Indah Delita Permatasari
Faculty of Electrical Engineering
Telkom University
Bandung, Indonesia
yoesindia@telkomuniversity.ac.id

Aloysius Adya Pramudita
Faculty of Electrical Engineering
Telkom University
Bandung, Indonesia
pramuditaadya@telkomuniversity.ac.id

Arnoldus Gratio Darryl Andyka
Faculty of Electrical Engineering
Telkom University
Bandung, Indonesia
arnoldusandyka@telkomuniversity.ac.i
d

Arif Abdul Aziz
Faculty of Electrical Engineering
Telkom University
Bandung, Indonesia
arifabdulaziz@telkomuniversity.ac.id

***Abstract* — Monitoring River water levels is a critical component of hydrological observation and early flood mitigation systems. Conventional monitoring approaches commonly rely on contact-based sensors, which require frequent maintenance and are vulnerable to environmental disturbances. To address these limitations, this study proposes a non-contact river water level monitoring system based on Frequency Modulated Continuous Wave (FMCW) millimeter-wave radar. The proposed system integrates an FMCW radar module with a Raspberry Pi as the central processing unit and is supported by a backup power supply to ensure continuous operation. The radar measures the distance between the sensor and the water surface, which is subsequently converted into water surface elevation information. Measurement data are processed in real time and transmitted to a cloud-based database, where they are visualized through a web-based monitoring interface. System evaluation includes functional testing of water level detection, power endurance assessment, and verification of data visualization and system performance. Experimental results demonstrate that the system is capable of detecting real-time variations in water surface elevation and maintaining operation during temporary power outages using the backup power supply. These results indicate that the proposed system is a viable alternative for non-contact and sustainable river water level monitoring and has potential for further development in hydrological monitoring and early flood mitigation applications.**

Keywords: FMCW radar, millimeter waves, water surface elevation, river monitoring, non-contact system.

I. INTRODUCTION

Flooding is one of the most frequent natural hazards affecting communities living along river basins, as observed in the Citarum River area, West Java, Indonesia [1]. This river frequently experiences overflow events, particularly during periods of high rainfall in the upstream region, resulting in flooding along its banks. Degradation of river control infrastructure and unplanned settlements that disregard land-use regulations further exacerbate flood risks. In addition, several areas in Bandung are located in low-lying regions, such as those along the Citarum and Cikapundung rivers, making them highly vulnerable to river overflow–induced flooding. High flow velocities following heavy rainfall may also trigger flash floods, posing significant risks to surrounding communities. Figure 1.1 illustrates the number of flood disaster events across cities and regencies in West Java from 2012 to 2022 [2].

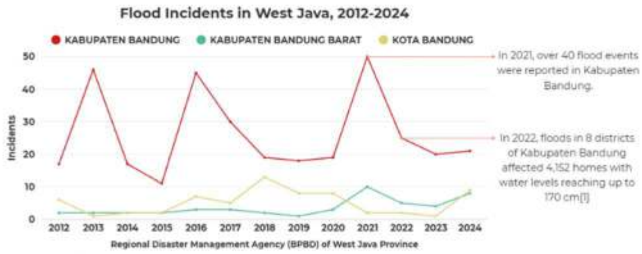

FIGURE 1
Flood Disaster Occurrences in West Java Cities and Regencies (2012–2022) [2]

According to data from the West Java Provincial Disaster Management Agency (BPBD), flood occurrences in Bandung Regency increased significantly in 2016 and 2021, with more than 40 flood events recorded in 2021 alone. In 2022, flooding affected several districts in Bandung Regency, including Soreang, Dayeuhkolot, Katapang, Baleendah, Cangkuang, Bojongsoang, Cicalengka, and Pameungpeuk, impacting 4,152 housing units with water depths ranging from 20 to 170 cm [3]. In contrast, data from the Bandung City Statistics Office (BPS) indicate no significant flood events in 2022, suggesting a lower flood incidence in Bandung City and West Bandung Regency compared to Bandung Regency [4].

Community-based flood monitoring initiatives, such as those conducted by the Cileungsi–Cikeas River Care Community (KP2C) using CCTV installations, highlight the urgent need for effective early warning systems [5]. Although camera-based monitoring provides visual information on potential flooding, it remains limited due to manual observation and lack of automation, underscoring the need for more integrated and automated solutions. Currently, river flow monitoring has begun to adopt various automated instruments, including sonar sensors and telemetry systems [6]. The Directorate General of Water Resources also provides online river monitoring platforms; however, the available information remains limited in terms of data update frequency and monitored parameters, thus reducing its effectiveness for early flood warning purposes [7].

Most existing telemetry-based monitoring systems primarily focus on water surface elevation as the sole parameter [8]. This approach has inherent limitations, as river flow conditions are influenced not only by water level but also by flow velocity, which may reach its peak at different times due to hydrodynamic effects [9]. Therefore, a monitoring system capable of simultaneously measuring water surface elevation and river flow velocity is required to provide a more comprehensive and responsive assessment of river conditions and flood potential.

II. METODOLOGY

A. *FMCW (Frequency Modulated Continous Wave)*

Frequency Modulated Continuous Wave (FMCW) signals are continuous radio-frequency signals whose instantaneous frequency is continuously varied over time [19]. The frequency variation follows a specific modulation pattern within a single modulation period, denoted as (T_c). This modulation enables the extraction of range and velocity information from the received signal.

One commonly used FMCW waveform is the sawtooth modulation, which exhibits a ramp-like frequency profile. In this waveform, the signal frequency is linearly increased from a minimum frequency (F_{min}), to a maximum frequency (F_{max}), during one modulation period, after which it is abruptly reset to (F_{min}). This process is repeated periodically to form a continuous sequence of frequency sweeps. The modulation process of the sawtooth FMCW signal is illustrated in Figure 2.1.

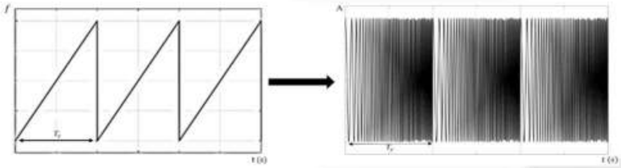

FIGURE 2
Modulation of the Sawtooth Signal [10].

B. *FMCW Method for Distance and Velocity Detection*

To detect range and velocity, FMCW radar operates based on the principle of transmitting a signal (Tx) and receiving the reflected signal (Rx) from a target. The received signal is a delayed and frequency-shifted version of the transmitted signal due to the propagation time and the motion of the target. The FMCW radar then performs a mixing process between the transmitted and received signals, resulting in an Intermediate Frequency (IF) signal.

The IF signal contains critical information related to the detected target. Specifically, it represents the frequency difference between the transmitted and received signals, which is directly correlated with the target's range [10]. In addition, the IF signal also includes frequency variations caused by the Doppler effect due to target motion, enabling velocity estimation [11]. The mixing process between the transmitted and received signals is illustrated in Figure 2.2.

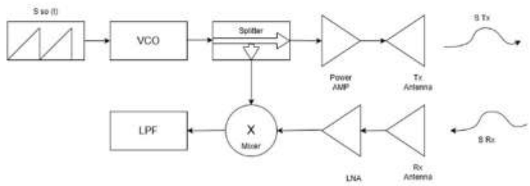

FIGURE 3
FMCW System Block Diagram [10]

1) *Beat Frequency*

The beat frequency is defined as the frequency difference between the transmitted waveform and the received waveform, which arises due to the propagation delay of the signal. The received signal experiences a time shift relative to the transmitted signal, resulting in a measurable frequency difference after the mixing process. This beat frequency can be analyzed to extract range information of the detected target.

The frequency difference between the transmitted and received signals is illustrated in Figure 2.3.

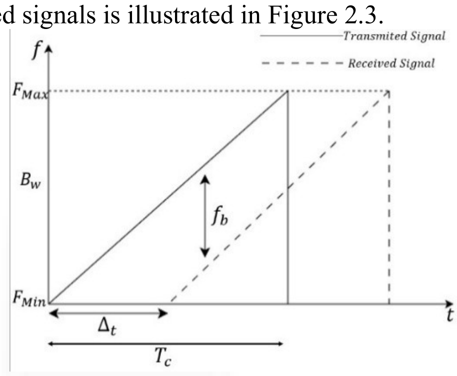

FIGURE 4
Visualization of the Frequency Difference Between Transmitted and Received Signals [10]

The frequency difference between the transmitted and received signals is referred to as the beat frequency, denoted as (f_b)[10]. The beat frequency has a direct correlation with the target range, which can be expressed by Equation below [19]:

$$X = \frac{f_b \cdot T_c \cdot c}{2 B_w}$$

where X represents the target range, T_c denotes the chirp duration (i.e., the period of one transmitted waveform), c is the speed of light, and B_w refers to the signal bandwidth.

2) *Doppler Frequency*

The Doppler frequency (f_d) refers to the frequency shift of the received signal caused by the relative motion of the target. When the target moves toward the radar, the received frequency increases, whereas when the target moves away from the radar, the received frequency decreases relative to the transmitted frequency.

The motion of the target affects the frequency of the signal received by the radar, as expressed in Equation below [8]:

$$Fr = \left(\frac{1 + \left(\frac{v}{c}\right)}{1 - \left(\frac{v}{c}\right)} \right) F$$

where v denotes the target velocity, c is the speed of light, Fr represents the received frequency, and F denotes the transmitted frequency.

Based on the above equation, the Doppler frequency can be derived as a function of the target velocity, the speed of light, and the transmitted frequency, as expressed in Equation below [8]:

$$f_d = \frac{2v}{c} . F$$

The detected Doppler frequency exhibits a linear correlation with the target velocity, provided that the target motion is not perpendicular to the radar line of sight. Therefore, an inclination in the radar depression angle, denoted by θ, must be considered. The Doppler frequency after angle correction is expressed in Equation below [8].

$$f_d = \frac{2vF}{c} \cos\theta$$

Accordingly, the equation can be rearranged to obtain the target velocity. The expression used to estimate the target velocity is given in Equation (2.5) [8].

$$v = \frac{f_d\, c}{2F \cos\theta}$$

C. Digital Signal Processing

Digital signal processing is a crucial stage in modern radar systems for converting raw data into meaningful information. In FMCW radar systems, this process involves several mathematical algorithms that transform signals from the time domain into the frequency domain to extract range and velocity information.

1) Fast Fourier Transform (Fast Time)

The primary process used for target range detection is the Fast-Time Fast Fourier Transform (FFT). The Fast-Time FFT converts the signal of a single chirp from the time domain into the frequency domain [9]. Based on the FMCW principle, there exists a direct relationship between the beat frequency (f_d) and the target range [10]. Consequently, the frequency spectrum produced by the FFT directly represents the distance of the observed target.

The highest amplitude peak in the FFT spectrum indicates the presence of the dominant target. The Fast-Time FFT processing is illustrated in Figure 2.4.

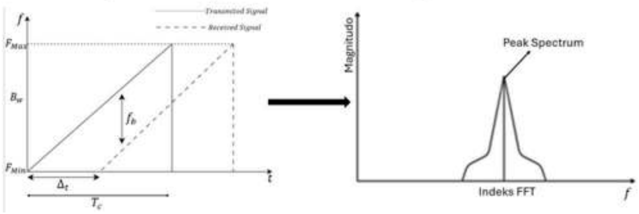

FIGURE 5
Frequency Difference Observed in the Fast-Time FFT Results

The FFT index represents the beat frequency (f_d) in the frequency domain.

2) Fast Fourier Transform (Slow Time)

The Slow-Time Fast Fourier Transform (FFT) is performed to detect target velocity. The Slow-Time FFT analyzes the magnitude and phase responses across consecutive chirps in the time domain. Continuous phase variations caused by target motion [12] are detected by the Slow-Time FFT as the Doppler frequency, denoted by (f_d). The Doppler frequency represents the rate of phase change in the frequency domain, and this process yields the dominant Doppler frequency corresponding to the target motion.

The Slow-Time FFT processing is illustrated in Figure 2.5.

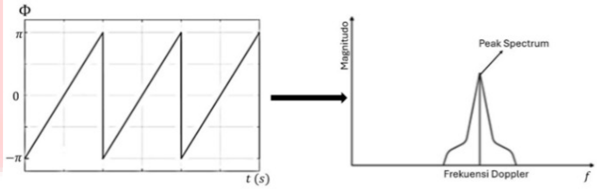

FIGURE 6
Phase Variation Observed in the Slow-Time FFT Process
Where Φ denotes the phase value.

3) Interpolasi Parabolik

Parabolic interpolation is a method based on the assumption that the peak of the magnitude spectrum exhibits a parabolic shape [13]. By analyzing the amplitude at the peak index (β) along with the amplitudes at the preceding index (α) and the succeeding index (γ), the true peak location can be mathematically estimated between discrete sample points. This technique has been shown to provide a more precise FFT index estimation.

The sampling process around the spectral peak is illustrated in Figure 2.6.

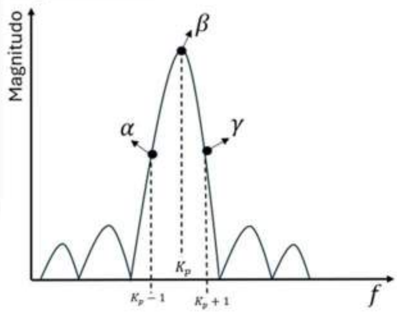

FIGURE 7
Sampling Process of the Parabolic Interpolation Method [13]
where K_p represents the peak index.

4) Nyquist's Theorem)

The Nyquist theorem states that, to reconstruct a continuous signal from its discrete samples without distortion, the sampling frequency must be at least twice the maximum signal frequency. In FMCW radar systems, the concept of sampling frequency differs across dimensions, namely Fast Time and Slow Time.

In the Fast-Time dimension, sampling is performed automatically by the hardware through the analog-to-digital converter (ADC). In contrast, in the Slow-Time dimension, the sampling frequency is entirely determined by the chirp rate, which corresponds to how frequently the system transmits chirps per second. Therefore, the sampling frequency used in the Slow-Time FFT is expressed in Equation below [14].

$$f_s = \frac{1}{\Delta t}$$

where f_s denotes the sampling frequency and Δt represents the time delay between consecutive chirps.

III. SYSTEM DESIGN

The FMCW radar component used in this study is the Universal Radar (uRAD), as this device is compatible as a processing unit and is equipped with educational support that facilitates the development stage. The acquired data are managed by both hardware (uRAD and Raspberry Pi) and software systems (Raspberry Pi using the Python programming language), through the signal processing procedures.

A. System Specifications

1) Hardware Specifications

The hardware system designed by the author using the uRAD is illustrated in Figure 4.4. This hardware system is equipped with several supporting components, including a Raspberry Pi, power outlet, USB cables, a cooling fan for air circulation, and an uninterruptible power supply (UPS) as a backup power source. The cooling fan operates at a voltage of 5 V, while the UPS provides a voltage of 12 V.

a) uRAD

The uRAD in this system functions as a radar sensor used to detect water flow velocity based on the Doppler principle. The device is connected to the Raspberry Pi via a USB Type-C port and transmits digital data for further analysis.

b) Raspberry Pi

The Raspberry Pi serves as the central control unit of the system. It receives data from the uRAD, processes the data, and transmits the results to the server. In addition, the Raspberry Pi manages the website interface.

c) UPS

The Uninterruptible Power Supply (UPS) acts as a backup power source. It receives a 12 V supply from the main electrical power and delivers power to the Raspberry Pi through a voltage converter that steps the voltage down to 5 V to meet power consumption requirements. By using a UPS, the system remains operational during power outages, ensuring that the detection of water surface level and flow velocity is not interrupted.

d) Electrical Power

This component refers to the main power outlet, which serves as the primary electrical power source for the system. Power is supplied to the UPS and subsequently distributed to Raspberry Pi and other devices. Without this component, the system cannot operate.

e) Cooling Fan

The cooling fan is used to maintain the operating temperature of the Raspberry Pi. It is connected via a USB port and operates at 5 V to prevent overheating during continuous system operation.

The detection of river water surface level and flow velocity is performed using an FMCW radar system, namely the uRAD (Universal Radar USB v1.2). This radar operates at a carrier frequency of 24.005 GHz with a bandwidth of 240 MHz, and a maximum number of samples per frame (Ns) of 200. The uRAD provides several operating modes; however, in this study, Mode 3 is selected. This mode enables simultaneous range and velocity detection using a triangular waveform while disabling the uRAD Moving Target Indicator (MTI) mode.

The uRAD is connected to a Raspberry Pi to execute the processing program. The data acquired from the uRAD consists of raw in-phase (I) and quadrature (Q) signals. The uRAD output corresponds to processed signals that have been filtered using a low-pass filter (LPF), represented in arbitrary units ranging from 0 to 4095. Figure 3.1 shows the physical appearance of the uRAD device from various perspectives.

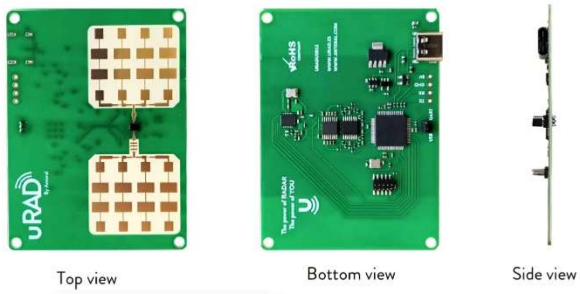

FIGURE 8
Views of uRAD from Multiple Angles

The uRAD is characterized by several RF parameters and specifications, as presented in Table 3.1.

TABLE 1
Parameters and Specifications of uRAD

Operating Conditions		
Parameter	***Value***	***Description***
Voltage	3,5 V – 10 V	5 V supplied via USB
Current	170 mA	-
Temperature	-20°C - 65°C	-
RF Parameters		
Frequency Bandwidth	24,005 GHz – 24,245 GHz	Pita frekuensi ISM
Output Power	19 dBm	EIRP (termasuk gain antena)
Gain Antena	16,6 dB	Antenna Array 4x4
Field of View	30° x 30°	-
Level Side Lobe	-19,8 dB – 21,3 dB	-

The Raspberry Pi used in this system has specifications as presented in Table 3.2.

TABLE 2
Raspberry Pi Specifications

Components	*Specifications*
Version	Raspberry Pi 3 Model B
Processor Chipset	BCM2837 64-Bit Quad-Core ARM Cortex-A53 Processor 1.2 GHz
RAM	1GB SDRAM @ 400 MHz
Ports	4 x USB 2.0 *type* A, 1 x HDMI, 1 x 3.5 mm *audio*, 1 x *micro*SD *card reader*
Networking	Wi-Fi 802.11n, Bluetooth 4.2, Ethernet
Dimension	85 x 56 x 17mm
Power	Micro USB socket 5V1, 2.5A

B. System Design

The selected solution for detecting river water surface level and flow velocity using the designed radar system is equipped with a protective enclosure and installed on a bridge, oriented toward the river surface as the observation target. The enclosure houses a Raspberry Pi responsible for processing the radar's received signals, as well as additional electrical components such as a UPS and a cooling system for the Raspberry Pi, as illustrated in Figure 3.2.

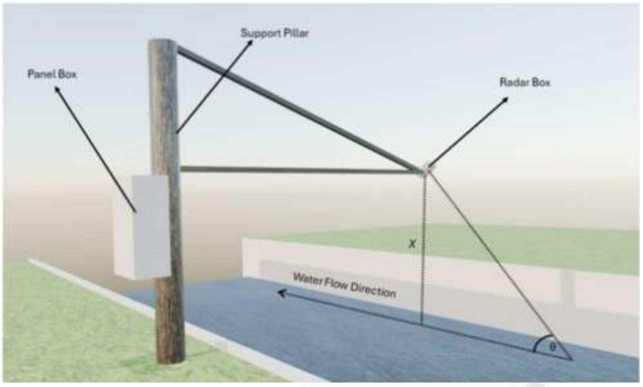

FIGURE 9
Hardware Installation Visualization

In this system, the uRAD radar is operated in Mode 2 (sawtooth), which enables periodic acquisition of range information and subsequent processing for flow velocity estimation. The acquired raw data consists of in-phase (I) and quadrature (Q) signals, which are then processed using two stages of the Fast Fourier Transform (FFT): the Fast-Time FFT for range estimation and the Slow-Time FFT for flow velocity estimation.

The radar parameters and configurations used in the signal processing are presented in Table 3.3.

TABLE 3
Radar Parameters and Configuration

Parameter	*Symbol*	*Value*	*Description*
Depression Angle	θ	70°	Surface Velocity Correction
Bandwidth	BW	240 MHz	Range Resolution Determination
Operating Frequency	Fc	24.005 GHz	uRAD Radar Frequency
Wavelength	λ	0.01249 m	$\lambda = \frac{c}{f} = \frac{3 \times 10^8}{24{,}005 \times 10^9}$
Chirp time	T_c	1 ms	Single Chirp Duration
Samples per Chirp	N	200	Range Resolution
Chirps per frame	Nc	256	Doppler Resolution
uRAD Mode	-	2	Sawtooth Mode for Range Acquisition

C. System Implementation

The implementation process carried out in this project aims to realize the previously proposed design into a functional prototype that can be used for detecting river water levels and flow velocity. The final solution consists of an integrated combination of hardware and software components. The results of the hardware implementation are presented in Figure 3.3.

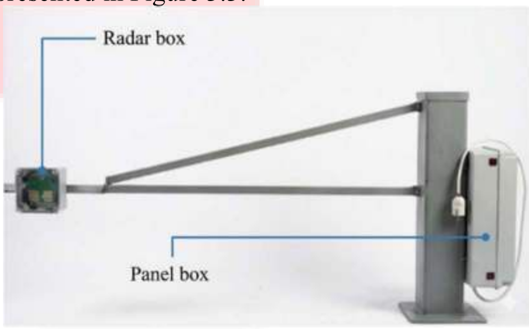

FIGURE 10
Hardware and Software Implementation

IV. RESULT AND ANALYST

The test results are divided into several sections, as previously described. The experimental data includes error rate and accuracy values, which can be calculated using the expression given in Equation below

$$Error\ Rate = \left|\frac{Detected\ Data - Actual\ Data}{Actual\ Data}\right| \times 100\%.$$

Subsequently, accuracy is obtained using the expression given in Equation (5.2).

$$Accuracy = 100\% - Error\ Rate.$$

A. Lab Scale

Laboratory-scale testing was conducted to validate the range detection results using the proposed method, which was designed to achieve higher range resolution and more detailed distance measurements.

FIGURE 11
Visualization of Laboratory-Scale Range/Height and Velocity Testing

The laboratory experiments were conducted using an aluminum reflector to represent the river water surface, as illustrated in Figure 4.1.

1) River Surface Elevation

The range testing was conducted with the radar set at a 70° depression angle, as shown in Figure 1.2. An aluminum foil reflector was used, and the reflector height was varied using a support structure to evaluate the distance measurement performance.

FIGURE 12
Range/Height Testing Conditions

Based on the experimental results, a comparative analysis was performed between the surface height obtained from manual measurements and the radar-based detection results. This comparison aims to evaluate the consistency of radar measurement trends with those of the reference method. Figure 4.3 presents the real range measurements and the corresponding radar detection results for each experimental trial.

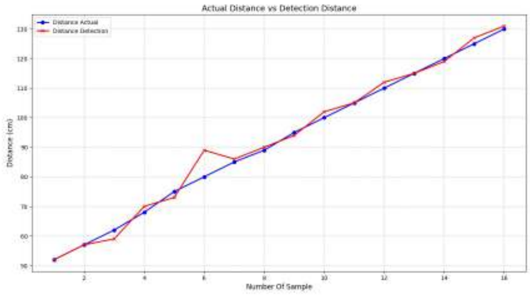

FIGURE 13
Comparison of Manual Measurement and Radar-Detected Range Results

The range test results obtained using the radar are summarized in quantitative parameters presented in Table 4.1, providing an overview of the system's detection accuracy.

TABLE 4
Average Range Detection Results

No.	*Parameter*	*Value*
1	Number of Trials	16
2	Average Accuracy	98%
3	Minimum Accuracy	95%
4	Maximum Accuracy	100%

Overall laboratory-scale detection results, validated using a reflector medium and a measuring tape as reference as shown in Figure 4.2, indicate that the proposed method achieves a relatively low error rate and can be effectively applied at a radar depression angle of 70°.

2) Flow Velocity Detection

Velocity testing was conducted with the radar set at a 70° depression angle to evaluate the reliability and suitability of the proposed method for estimating river flow velocity under realistic conditions. An aluminum foil reflector was moved at varying speeds, and the accuracy of the detected velocity is illustrated in Figure 4.4.

FIGURE 14
Velocity Testing Conditions

The graph in Figure 4.5 presents a comparison between manual velocity measurements and radar-based velocity detection for each trial, allowing the gradual variation in velocity to be clearly observed.

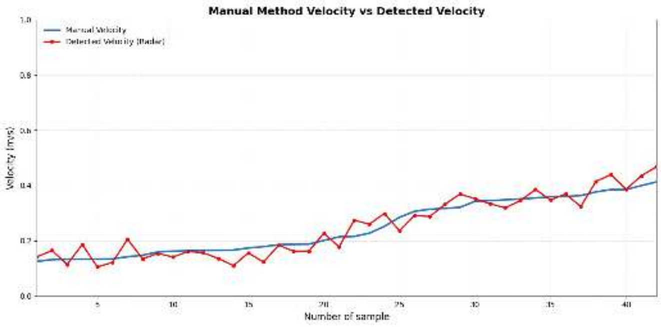

FIGURE 15
Velocity Comparison between Manual Measurements and Radar-Based Detection

Furthermore, the test results are summarized in terms of average accuracy in Table 4.2, providing an overview of the system performance in velocity detection.

TABLE 5
Average Velocity Detection Results

No.	***Parameter***	***Value***
1	Number of Trials	42
2	Average Accuracy	87%
3	Minimum Accuracy	55%
4	Maximum Accuracy	100%

B. *Small River Scale*

The small-scale river testing was conducted to verify the proposed method prior to full-scale field implementation. Figure 4.6 shows the documentation of the data acquisition process during the small-scale river test, where a measuring tape was used as a staff gauge (phale scale) and to measure the travel distance for velocity assessment using the float method.

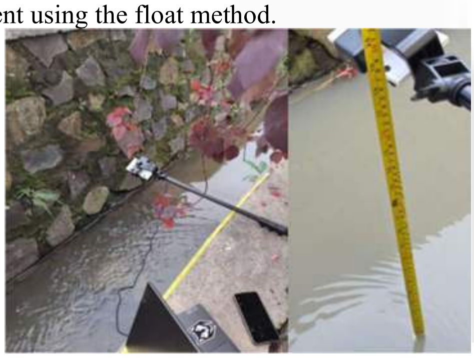

FIGURE 16
Small-Scale River Testing

1) River Surface Elevation

The water surface elevation data are obtained by subtracting the radar-detected distance to the river water surface from the radar-to-riverbed distance. Since the river water level cannot be controlled, data were collected at different time intervals to validate the detection results.

TABLE 6
Small-Scale River Water Level Test Data

Water Level Test Data at Small Scale River				
Experiment No.	***Actual Distance***	***Detected Distance***	***Error rate***	***Accuracy***
1	0	0	0%	100%
2	12	10	17%	83%
3	20	20	0%	100%
4	30	30	0%	100%
5	40	38	5%	95%
Average			4,4%	95,6%

Table 4.3 presents the detection results validated by measuring the water surface elevation using a measuring tape, as shown in Figure 4.6. The water level measurement was performed using the parabolic interpolation method, which depends on the magnitude values of the received signal. Variations in the water surface conditions cause fluctuations in the magnitude values, which in turn affect the estimated water level.

To mitigate this effect, data was collected over a duration of 15 seconds and subsequently averaged to obtain the detection results presented in Table 4.5.

2) Flow Velocity Detection

River flow velocity data were acquired by collecting samples over a duration of 15 seconds. The extracted data were then averaged to obtain the detected flow velocity. The detection results were verified using the float method as a reference, which has a tolerance range of approximately 10–20%.

TABLE 7
Small-Scale River Flow Velocity Test Data

Water Level Test Data at Small Scale River				
Experiment No.	***Float Velocity (m/s)***	***Detected Velocity (m/s)***	***Error rate***	***Accuracy***
1	0,145	0,1176	18,90 %	81,10%
2		0.1160	20%	80%
3		0.1269	12,48 %	87,52%
4		0.1006	30,62 %	69,38%
5	0,202	0,1877	7,08%	92,92%
6		0,2025	0,25%	99,75%
7		0,1869	7,48%	92,52%
8		0,1777	12,03 %	87,97%
Average			13,60 %	86,40%

The radar-detected velocity is updated at sub-second intervals; therefore, the detected velocity is obtained by averaging multiple data samples collected over a 15-second measurement period. Similarly, the reference velocity measured using the comparison method is also derived from the average of several samples. As shown in Table 4.4, the overall accuracy of the velocity detection is 86.40%.

C. *Big River Scale*

Primary testing was conducted at the Cidurian River under small-scale river conditions to verify the proposed method prior to deployment in the actual implementation environment. The testing setup is illustrated in Figure 4.3.

FIGURE 17
Implementation at the Cidurian River

Figure 4.7 shows the documentation of the data acquisition process conducted at the Cidurian River on a small-scale setup. A measuring tape was used to determine the travel distance for velocity measurement using the float method, and a staff gauge provided by the Cidurian River management was used for water level reference.

1) *River Surface Elevation*

The water surface elevation data was obtained using the same method as the small-scale river water level calculation described previously. In this test, measurements were performed in 30-second loops, with the averaging of variables conducted over the last 15 seconds of each measurement interval.

TABLE 8
Cidurian River Water Level Test Data

Water Surface Elevation Data at the Cidurian River					
Experiment No.	***Sampling Time***	***Actual Distance***	***Detected Distance***	***Error rate***	***Accuracy***
1	14:17	0.14	0.14	21%	79%
2	14:18	0.136	0.136	19%	81%
3	14:18	0.1382	0.1382	20%	80%
4	14:19	0.1415	0.1415	22%	78%
5	14:19	0.1404	0.1404	22%	78%
6	14:19	0.1418	0.1418	22%	78%
7	14:20	0.13	0.13	15%	85%
8	14:20	0.1218	0.1218	10%	90%
9	14:20	0.1456	0.1456	24%	76%
10	14:21	0.1367	0.1367	20%	80%
11	14:21	0.1326	0.1326	17%	83%
12	14:21	0.1381	0.1381	20%	80%
13	14:22	0.1344	0.1344	18%	82%
14	14:22	0.1495	0.1495	26%	74%
15	14:23	0.114	0.114	4%	96%
Average				18,67%	81,33%

Table 4.5 presents the results of water level detection validated using the *phale scale* available at the implementation site, as shown in Figure 4.7. In this experiment, the radar installation height ranged from 11 to 14 cm. Fluctuations in the detected water level were observed, which are primarily caused by using the parabolic interpolation method that relies on magnitude values at neighboring indices. In addition, the continuously moving water surface results in fluctuating reflected signal magnitudes, making it difficult to achieve 100% measurement accuracy for the water level.

2) *Flow Velocity Detection*

River flow velocity data were collected by acquiring samples over a duration of 15 seconds. The extracted data were then averaged over this 15-second interval to obtain the detected river flow velocity. The detection results were subsequently validated using the float method as a reference, which has an acceptable tolerance range of 10–20%.

TABLE 9
Cidurian River Flow Velocity Test Data

Water Surface Elevation Data at the Cidurian River					
Experiment No.	***Sampling Time***	***Float Velocity (m/s)***	***Detected Velocity (m/s)***	***Error rate***	***Accuracy***
1	14:17	0.1995	0.2561	22%	78%
2	14:18	0.1995	0.241	17%	83%
3	14:18	0.1995	0.2331	14%	86%
4	14:19	0.1995	0.2185	9%	91%
5	14:19	0.1995	0.3007	34%	66%
6	14:19	0.1995	0.2243	11%	89%
7	14:20	0.1995	0.2637	24%	76%
8	14:20	0.1995	0.2473	19%	81%
9	14:20	0.1995	0.2586	23%	77%
10	14:21	0.1995	0.2206	10%	90%
11	14:21	0.1995	0.2227	10%	90%
12	14:21	0.1995	0.2621	24%	76%
13	14:22	0.1995	0.2129	6%	94%
14	14:22	0.1995	0.2363	16%	84%
15	14:23	0.1995	0.2591	23%	77%

Water Surface Elevation Data at the Cidurian River					
Experiment No.	***Sampling Time***	***Float Velocity (m/s)***	***Detected Velocity (m/s)***	***Error rate***	***Accuracy***
Average				17,47%	82,53%

Table 4.6 above shows the radar detection results for the river flow velocity variable. The detected velocity values are obtained from the average calculation of approximately ±600 samples collected over a 15-second interval. The float method, used as a reference for validation, is also derived from several observation samples to minimize errors caused by human observation. Based on the results, the average accuracy level of the velocity measurement in the Cidurian River is 82.53%.

D. Analysis of Test Results

Based on the experiments conducted, the system can detect river water level and flow velocity within the predefined accuracy thresholds. However, several data samples exhibit accuracy levels below the threshold, which are likely caused by suboptimal radar deployment during implementation, affecting detection performance. In addition, the velocity measurement validation is limited, as flow velocities exceeding 0.45 m/s were not tested. Consequently, the system performance at higher flow velocities has not yet been fully validated.

V. Conclusion

Before you begin to format your paper, first write and save the content as a separate text file. Complete all content and organizational editing before formatting. Please note sections A-D below for more information on proofreading, spelling and grammar.

References

[1] M. Elgana Mubarokah and D. Olivier Purba, “Dayeuhkolot Bandung Kembali Banjir Senin Malam, Rendam Belasan Kampung,” Kompas.com, Bandung, Feb. 25, 2025. [Online]. Available: https://bandung.kompas.com/read/2025/02/25/195628278/dayeuhkolot-bandung-kembali-banjir-senin-malam-rendam-belasan-kampung?utm_source=Various&utm_medium=Referral&utm_campaign=Top_Desktop

[2] Badan Penanggulangan Bencana Daerah, “Jumlah Kejadian Bencana Banjir Berdasarkan Kabupaten/Kota di Jawa Barat,” Bandung, 2025. [Online]. Available: https://opendata.jabarprov.go.id/id/dataset/jumlah-kejadian-bencana-banjir-berdasarkan-kabupatenkota-di-jawa-barat

[3] Pusat Krisis Kesehatan Kemenkes RI, “Informasi Awal Banjir di 8 Kecamatan, Bandung, Jawa Barat,” Bandung, 2022. [Online]. Available: https://pusatkrisis.kemkes.go.id/Banjir-di-BANDUNG-JAWA-BARAT-22-10-2022-7

[4] BPS Kota Bandung, “Kota Bandung Dalam Angka,” Bandung, 2025. [Online]. Available: https://ppid.bandung.go.id/storage/ppid_utama/7SlqumeHvY7YmTBfe7hkKSpyGjLeJzbTdOwfCM5j.pdf

[5] M. F. Setiawan, “KP2C pasang CCTV di Sungai Cileungsi-Cikeas untuk deteksi dini banjir,” Antara News, Bogor, Jul. 06, 2022. [Online]. Available: https://www.antaranews.com/berita/2981397/kp2c-pasang-cctv-di-sungai-cileungsi-cikeas-untuk-deteksi-dini-banjir

[6] Highertech, “Telemetry Specialist - Solusi Peralatan Telemetri,” higertech.com. [Online]. Available: https://higertech.com/

[7] BBWS Citarum, “Tabel Monitoring Balai Besar Wilayah Sungai Citarum,” opbbwscitarum.higertech.com. [Online]. Available: https://opbbwscitarum.higertech.com/Home/TabelMonitoringR. Nicole, “Title of paper with only first word capitalized,” J. Name Stand. Abbrev., in press.

[8] “Doppler Effect: Transforming Radar Technology,” Memoracad. [Online]. Available: https://mecorad.com/doppler-effect-transforming-radar-technology/

[9] A A Pramudita, “Multi Pulse CW Dopper Radar,” Telkom University, Bandung.

[10] F. I. H. Chang, “Sistem Pengukur Kecepatan Arus Air Menggunakan Current Meter Tipe ‘1210 AA,’” *Jurnal Teknik Sipil (Neliti)*, vol. 19, p. 15, 2017, [Online]. Available: https://media.neliti.com/media/publications/271542-sistem-pengukur-kecepatan-arus-air-mengg-f12fcb2a.pdf

[11] A A Pramudita, “3. Bentuk Gelombang,” *Telkom University, Bandung*.

[12] D. G. M. John G. Proakis, *Digital Signal Processing, 4e*. Hoboken, NJ: Pearson Prentice Hall, 2007.

[13] Mark A. Richards, *Fundamentals of Radar Signal Processing*, 2nd Editio. New York: McGraw-Hill Education, 2014. [Online]. Available: https://zlib.pub/book/fundamentals-of-radar-signal-processing-4hg9j4vj7oj0

[14] C. Candan, “Fine Doppler Estimation in Pulse-Doppler Radar,” *IEEE Signal Process Lett*, vol. 18, no. 6, 2011, doi: 10.1109/LSP.2011.2143690.